Published in final edited form as:
J Am Chem Soc. 2010 August 25; 132(33): 11504–11509. doi:10.1021/ja101961x.

Natural-Abundance ^{43}Ca Solid-State NMR Spectroscopy of Bone

Jiadi Xu[a], **Peizhi Zhu**[b], **Zhehong Gan**[c], **Nadder Sahar**[d], **Mary Tecklenburg**[e], **Michael D. Morris**[b,*], **David H. Kohn**[d], and **Ayyalusamy Ramamoorthy**[a,*]

[a] Department of Biophysics, University of Michigan, Ann Arbor, MI 48109-1055

[b] Department of Chemistry, University of Michigan, Ann Arbor, MI 48109-1055

[c] National High Magnetic Field Lab, Tallahasse, FL

[d] Department of Biomedical Engineering, University of Michigan, Ann Arbor, MI 48109-1055

[e] Department of Chemistry, Central Michigan University, Mt. Pleasant, Michigan

Abstract

Structural information about the coordination environment of calcium present in bone is highly valuable in understanding the role of calcium in bone formation, biomineralization, and bone diseases like osteoporosis. While a high-resolution structural study on bone has been considered to be extremely challenging, NMR studies on model compounds and bone minerals have provided valuable insights into the structure of bone. Particularly, the recent demonstration of ^{43}Ca solid-state NMR experiments on model compounds is an important advance in this field. However, application of ^{43}Ca NMR is hampered due to the low natural-abundance and poor sensitivity of ^{43}Ca. In this study, we report the first demonstration of natural-abundance ^{43}Ca magic angle spinning (MAS) NMR experiments on bone, using powdered bovine cortical bone samples. ^{43}Ca NMR spectra of bovine cortical bone are analyzed by comparing to the natural-abundance ^{43}Ca NMR spectra of model compounds including hydroxyapatite and carbonated apatite. While ^{43}Ca NMR spectra of hydroxyapatite and carbonated apatite are very similar, they significantly differ from that of cortical bone. Raman spectroscopy shows that the calcium environment in bone is more similar to carbonated apatite than hydroxyapatite. A close analysis of ^{43}Ca NMR spectra reveals that the chemical shift frequencies of cortical bone and 10% carbonated apatite are similar but the quadrupole coupling constant of cortical bone is larger than that measured for model compounds. In addition, our results suggest that an increase in the carbonate concentration decreases the observed ^{43}Ca chemical shift frequency. A comparison of experimentally obtained ^{43}Ca MAS spectra with simulations reveal a 3:4 mole ratio of Ca-I:Ca-II sites in carbonated apatite and a 2.3:3 mole ratio for hydroxyapatite. 2D triple-quantum ^{43}Ca MAS experiments performed on a mixture of carbonated apatite and the bone protein osteocalcin reveal the presence of protein-bound and free calcium sites, which is in agreement with a model developed from X-ray crystal structure of the protein.

Introduction

Bone is a complex composite material system with a hierarchial structure. The composition can be divided into two major components: an organic matrix and an inorganic mineral that interact with each other and contribute to bone mechanical properties and to its other functions including calcium homeostasis.1 The organic matrix is about 90% type I collagen.

*Corresponding Author: Ayyalusamy Ramamoorthy, Phone: 734-647-6572, Fax: 734-763-2307, ramamoor@umich.edu.

Supporting Information Available: Raman spectra and simulated ^{43}Ca NMR spectra of bone and model compounds. This material is available free of charge via the Internet at http://pubs.acs.org.

The remainder consists of about 200 non-collagenous proteins, which incude proteins that regulate biomineralization, bone formation and bone resorption, and proteins that chemically couple the mineral and matrix. Bone mineral is a poorly-crystalline carbonated hydroxyapatite, which also contains small amounts of other cations and anions. The crystallites are small, typically less than 20 nm in the c-axis direction, and shorter in the a- and b-axes. Arguably, the mineral could better be described as an apatite-like material.2

Understanding the molecular organization of bone at a high-resolution is of considerable current importance as it would provide valuable insights into the role of individual components on the strength and toughness of bone and could also provide a better understanding of degenerative joint diseases like osteoarthritis. However, this is a daunting task, because bone presents a significant challenge to many commonly used physical techniques. Solid-state NMR spectroscopy is an excellent tool to obtain such high-resolution information on bone samples not subjected to any chemical pretreatment (e.g. deproteination or demineralization). In fact, ^{1}H, ^{13}C ^{31}P, and 2D ^{1}H/^{31}P HETCOR NMR experiments3–21 under magic angle spinning (MAS) conditions have been used for the structural studies of bone mineral and model calcium phosphate compounds. These studies have provided a wealth of atomic-level information from model compounds and considerably enhanced our understanding on the structure of bone. ^{31}P MAS NMR experiments are insensitive to structural changes in bone mineral and have provided relatively little information about either biomineralization or the formation of bone mineral.10, 21 On the other hand, proton MAS NMR has been used to establish the presence of a hydroxide ion in the c-axis column of bone mineral at 20% of the amount found in hydroxyapatite and also to distinguish among different types of water in the mineral lattice.3–5,9 However, it remains a major challenge to understand the chemical environment around calcium ions in the bone matrix.

Knowledge of the storage and transport of calcium ions in bone, and the interaction between bone proteins and calcium ions is essential for understanding biomineralization and bone remodeling. Moreover, the calcium ions at the surfaces of mineral crystallites are likely the sites for chelation that couples mineral to matrix, although the chelating proteins are still unknown. Additionally, these ions tightly bind bisphosphonates as sparingly soluble salts and allow bisphosphonate antiresorptives to be administered at intervals varying between one week and one year, depending on the solubility.22

Unlike other techniques such as X-ray diffraction and neutron diffraction20, NMR parameters measured from a ^{43}Ca MAS experiment provide a direct high-resolution observation of the environment around the calcium ion. Therefore, ^{43}Ca solid-state NMR spectroscopy could be a powerful tool to study the mechanisms by which non-collagenous proteins and other molecules, that may chelate calcium such as lipids, guide biomineralization, bone formation, bind mineral to matrix and control the delivery of therapeutic molecules. ^{43}Ca chemical shift is sensitive to the environment around the calcium ion. A 50 ppm high-field shift relative to the free Ca^{2+} ion in solution has been observed for Ca^{2+} bound to bovine testis calmodulin23. ^{43}Ca NMR has been previously used to identify and characterize the Ca^{2+} binding sites, and to study the transport process in other proteins including calmodulin, calbindin, troponin C and parvalbumin23–31. ^{43}Ca MAS experiments have also been used to obtain structural information from inorganic solids32–38. However, there are several factors that limit the application of ^{43}Ca solid-state NMR to bone specimens. Low gyromagnetic ratio and natural-abundance (0.145%) of ^{43}Ca quadrupolar nucleus (nuclear spin 7/2) with a low resonance frequency (for example, it is 33.5 MHz in a 11.7 T magnetic field) make a bone sample considerably less sensitive (than natural-abundance ^{13}C for example) and therefore unsuitable for NMR spectroscopy. Therefore, ^{43}Ca NMR until recently has not been considered for studies on biological systems without isotope enrichment. The second-order quadrupole moment of ^{43}Ca cannot

be averaged out under MAS, which could further reduce the sensitivity and spectral resolution. Fortunately, the second-order quadrupolar broadening of ^{43}Ca NMR is relatively small in most inorganic and organic solids32–38, and recent studies on model calcium phosphate compounds have demonstrated its potential applications. In this study, natural-abundance ^{43}Ca MAS experiments are demonstrated for the first time on bone tissue specimens and used to analyze the effect of deproteination of cortical bone.

Raman spectroscopy is another useful tool for studying heterogeneous materials such as bone and other mineralized tissues. The information obtained from Raman spectroscopy is less detailed than that provided by NMR, but can be acquired quickly, and, if needed, with spatial resolution on the micron scale. The phosphate band ~ 959 cm^{-1} is a prominent marker for mineral content in bone and other phosphate and carbonate bands are monitors of subtle changes in mineral composition. Amide I, amide III, and CH_2 deformation bands are typical markers for the protein and other organic matrix components of bone.39–44 Even in cases where it is difficult to pinpoint the structural changes that cause shifts in Raman band positions or intensities, their presence indicate subtle changes that may be fruitfully studied by NMR spectroscopy. Therefore, in this work, ^{43}Ca solid-state NMR has been employed to study the structure of bovine cortical bone. In addition, we have shown that a combination of a high external magnetic field and a 2D MQMAS technique can provide high-resolution information about the coordination chemistry around the calcium atom present in bone. We have chosen several systems that illuminate features of cortical bone, including bovine cortical bone, deproteinated bovine cortical bone, synthetic carbonated apatite and hydroxyapatite, and synthetic ^{43}Ca-enriched carbonated apatite. The ^{43}Ca-enriched carbonate apatite with absorbed bovine osteocalcin is used in this study as a model complex for the first ^{43}Ca NMR studies of the interaction between bone mineral and a matrix protein.

Materials and Methods

Materials

Cortical bone powder, deproteinated bone powder, hydroxyapatite, and synthetic carbonated apatite were used in our study. Hydroxyapatite was purchased from Sigma-Aldrich Company.

Bovine femora were harvested from freshly slaughtered animals (2–4 years old) obtained from a local slaughterhouse. Femora were stripped of soft tissue, and cortical bone specimens were prepared from central diaphyseal sections. Each diaphysis was sectioned on a band saw into parallelepipeds. Calcium-buffered saline was used during all machining steps to avoid heating the bone and to maintain tissue saturation and ionic balance. Parallelepipeds randomly chosen from an inventory of 10 femora with respect to longitudinal and circumferential location were milled into a powder cryogenically cooled with liquid nitrogen.

Bone powder was deproteinated with hydrazine according to a published procedure.43 Briefly, 2g of bovine bone powder was immersed directly into 20 mL of hydrazine (95%, Sigma Aldrich) and stirred at 55 °C in a glass bottle for 1 hour. Then the temperature was increased to 60 °C. After 4 hours of reaction, the sample was washed with water then ethanol to remove supernatant. After drying at 37 °C for 1 hour, the sample was immersed into 10 mL of hydrazine and stirred at 60 °C for 19 hours to completely remove all remaining proteins and collagen and then rewashed with water and ethanol, and finally dried at 37 °C for 1 hour.

Synthetic B-type carbonated apatite samples were prepared according to a published procedure40 and dried overnight at 100 °C. Weight percent carbonate was determined by

infrared spectroscopy calibrated against carbonated apatite standards analyzed coulometrically (Galbraith Labs, Knoxville, TN).40 Carbonated apatite samples contained 5.6 wt% carbonate.

Bovine osteocalcin adsorption to ^{43}Ca carbonated apatite

^{43}Ca carbonated apatite was prepared from calcium-43 carbonate (57.9% enrichment, Cambridge Isotope Laboratories, Massachusetts, USA) according to the following procedure: 30.4 mg of calcium carbonate (^{43}Ca, 57.9% enriched) was dissolved in 1.5 mL of 0.5 M nitric acid. Dry, filtered nitrogen was bubbled into the solution for several minutes to reduce dissolved CO_2. A second solution (13.4 mg $(NH_4)_2HPO_4$, 1.20 mL water, 0.90 mL of NH_4OH) was added dropwise to the calcium carbonate solution which was maintained at 80 °C in a water bath. After 30 minutes the solution was cooled to room temperature, centrifuged (5 min, 3400 rpm), and supernatant was removed. The pellet was washed with 5 mL water and centrifuged five times and then the pellet was dried overnight at 80 °C.

Bovine osteocalcin (Haematologic Technologies, Vermont, USA) was physisorbed to ^{43}Calcium carbonated apatite by mixing a solution composed of 0.1 mg/mL of osteocalcin in a phosphate buffer with about 20 mg of ^{43}Calcium-enriched carbonated apatite. After 6h of mixing under mild stirring at −4 °C, the unbound protein was separated from the protein-apatite complex through centrifugation. The protein-apatite sample was washed several times with buffer and was packed in the rotor for ^{43}Ca solid-state NMR studies.

NMR spectroscopy

Solid-state NMR experiments were performed on a Bruker 833 MHz NMR spectrometer at the national high-magnetic field laboratory (NHMFL, Tallahassee, Florida). A single channel 4 mm MAS probe tuned to 55.8 MHz and a 4 mm zirconia rotor were used in the 833 MHz spectrometer with a 10 kHz spinning speed. ^{43}Ca chemical shift spectra are referenced with respect to to $CaCl_2/H_2O$ saturated solution at 0 ppm. All spectra were processed using the Topspin software from Bruker. Other experimental details are given in the figure caption.

Results and Discussion

Natural-abundance ^{43}Ca solid-state MAS NMR spectroscopy of cortical bone is feasible

^{43}Ca MAS experiments were performed on powder samples of bovine cortical bone, deproteinated bone, carbonated apatite and hydroxyapatite. Natural-abundance ^{43}Ca spectra of these samples are given in Figure 1 along with experimental conditions. It is impressive that a natural-abundance ^{43}Ca NMR spectrum of cortical bone with a reasonable signal-to-noise ratio (9.5) is obtainable within 36 hours of data acquisition. The frequency and lineshape of ^{43}Ca spectral lines indicate the nature and number of coordination of Ca in the sample. Any changes in the line shape suggest a change in the coordination chemistry at the calcium site.

Differences between cortical bone and synthetic carbonated apatite around Ca sites revealed by ^{43}Ca NMR

The two observed peaks at 2 and 14 ppm in the ^{43}Ca NMR spectrum of a powder sample of hydroxyapatite (Figure 1a (second column) and Table 1) indicates two different coordination environments around calcium, which corroborates with previous studies.36–37 The NMR parameters, chemical shift, δ, quadrupole coupling constant, C_Q, and the asymmetry parameter, η_Q, associated with each calcium site were determined from computer simulations via quadfit.45 Experimentally measured values of C_Q and η_Q reported from previous studies were used in our simulations for the model compounds, carbonated apatite

and hydroxyapatite. The results are given in Table 1 and the simulated spectra are shown as dashed lines in Figure S2. The simulated spectra agree reasonably well with the experimental results. For the purpose of clarity, simulated spectra of Ca-I and Ca-II are also potted in Figure 1 (second and third columns). The intensity ratio of Ca-I:Ca-II was determined to be 2.3:3 for hydroxyapatite (Figure 1a (second column)) and 3:4 for 5% carbonated apatite (Figure 1b (second column)). The lineshape of carbonated apatite is significantly broader compared to pure hydroxyapatite, which can be attributed to the presence of CO_3^{2-} ions. Since ~7 % of carbonate ions are present in bone, the observed carbonate-induced change in the ^{43}Ca NMR spectral line shape is interesting and could be an important parameter to understand the environment of calcium in bone. Therefore, to further understand the role of carbonate ions on the ^{43}Ca NMR line shape, carbonated apatite samples with varying amounts of carbonate ions were prepared and their ^{43}Ca NMR are shown in Figure 1 (first column). The difference in the S/N ratio observed between these spectra is mainly due to the difference in the amount of samples used in NMR experiments. Nevertheless, judging from these spectra (except spectra f and g that have poor S/N ratio) the ^{43}Ca NMR lineshape broadens as the concentration of carbonate ion increases. A comparison of experimental and simulated spectra from 5 and 10 % carbonated samples indicates a small change in the isotropic chemical shift value (about 2 ppm; see Table 1) and also a 2.3:3 intensity ratio between Ca-I and Ca-II sites for the 10% carbonated sample. Interestingly, the quadrupole coupling constant values obtained from these carbonated and non-carbonated (that is hydroxyapatite) samples are the same within the limitation of experimental measurements (Table 1). These results suggest that the coordination geometry in hydroxyapatite and carbonated apatite samples are similar while the chemical difference between coordinating ligands (phosphate vs carbonate) contribute to the observed difference in the chemical shift.

In contrast, ^{43}Ca resonances corresponding to Ca-I and Ca-II sites observed from the cortical bone sample (Figure 1e (second column)) is shifted to higher field region from that of model compounds, hydroxyapatite (Figure 1a (second column)) and carbonated apatite (Figures 1b & c (second column)). The characteristic peak of Ca-II in all model compounds (observed in the 10–14 ppm range in Figures 1a,b,c (second column) and Table 1) was not observed in the ^{43}Ca NMR spectrum of cortical bone. These results suggest that the coordination environment of calcium in bone mineral material differs from that of synthetic hydroxyapatite or carbonated apatite compounds. However, it is difficult to correlate the observed changes with the possible difference in the coordination chemistry around calcium sites between cortical bone and model compounds. Further, these observations cannot be solely explainable by the observed line broadening of ^{43}Ca NMR signal as demonstrated by the simulations (see Figure S2). The dependence of the observed ^{43}Ca NMR line shape on the quadrupole coupling constant C_Q and the line broadening factor is illustrated in simulated spectra as shown in Figure S2, where the asymmetry parameter, η_Q, was assumed to be a constant. Based on the simulated spectra, the large resonance shift and the disappearance of Ca-II peak in the cortical bone spectrum (Figure 1e (second column)) could be explained using a large quadrupole coupling constant C_Q. By assuming the line broadening in the cortical bone sample to be the same as that observed for 10% carbonated apatite sample, a C_Q value of 4 MHz was obtained for the cortical bone sample. The chemical shift values of Ca-I and Ca-II were also determined by comparing the experimental and simulated spectra and are very close to that observed for 10 % carbonated apatite (Table 1). These chemical shift values suggest the presence of carbonate ions around the calcium sites in cortical bone, which is consistent with previous reports on the presence of ~7 % carbonate ions in the bone matrix.41 On the other hand, a large quadrupole coupling constant (C_Q=4 MHz) observed from cortical bone could be attributed to the poor crystalline nature of the bone mineral sample as compared to carbonated apatite samples. In addition, interaction between calcium and a protein in bone could also contribute to the observed

difference in quadrupole coupling values between these samples. This interpretation is consistent with a model proposed from a crystallography study on porcine osteocalcin which revealed the coordination of negatively charged side chains of aspartic acid and carboxylated glutamic acid residues with calcium in a hydroxyapaptite crystal lattice.47 In this context, our results indicate that the ^{43}Ca quadrupole coupling constant is highly sensitive to protein-calcium binding in bone. Therefore, the use of MAS NMR experiments to measure ^{43}Ca quadrupole coupling constant could provide insights into the recognition of the bone mineral by proteins in the biological processes of bone.

The use of ^{43}Ca NMR to obtain high-resolution insights into the nature of protein-calcium interactions is severely limited by the poor S/N observed from bone samples. However, we have made the first attempt to use ^{43}Ca NMR experiments to probe the chemical nature of the interaction between a bone protein and bone minerals. For this purpose, we prepared two different samples: the first sample (denoted as deproteinated bone sample) was prepared by removing all proteins from a cortical bone powder sample while the second sample (denoted as osteocalcin-bone sample) was prepared by mixing osteocalcin with a ^{43}Ca-enriched carbonated apatite. The natural abundance ^{43}Ca NMR of the deproteined bone sample is shown in Figure 1d (second column). While the S/N ratio of the deproteinated bone sample is low (Figure 1d (second column)), the frequency distribution of the spectral line more closely resembles that of the untreated cortical bone (Figure 1e (second column)) than that of the model compounds (Figures 1a–c (second column)). The low S/N ratio is due to the less sample volume used to obtain this spectrum when compared to other samples.

Triple-quantum ^{43}Ca solid-state MAS NMR provides evidence for osteocalcin binding to calcium sites

A one-dimensional natural-abundance ^{43}Ca MAS spectrum of 5% carbonated apatite is given in Figure 1b (second column) while that of a mixture of bone protein osteocalcin and ^{43}Ca-enriched carbonated apatite is shown in Figure 2a (solid line spectrum). A simulated spectrum that fits well with the experimental spectrum of 5% carbonated apatite sample (see the simulated spectrum given in dashed lines in Figure 1b (second column)) is also shown in Figure 2a (dashed lines spectrum) for a comparison. From the comparison of the simulated and experimental spectra in Figure 2a, it is clear that the addition of bone protein osteocalcin to carbonated apatite significantly broadens the ^{43}Ca NMR spectrum and also generates some extra peaks in the spectrum as the spectrum is shifted high field. The observed line broadening in ^{43}Ca MAS spectra may in general be attributed to the unaveraged higher-order quadrupole coupling interaction. Therefore, to achieve a better resolution on the ^{43}Ca NMR spectrum of the carbonated apatite sample containing osteocalcin, a 2D triple-quantum MAS (3QMAS) experiment46 was performed and the resultant spectrum is shown in Figure 2b. Since natural-abundance ^{43}Ca 2D NMR experiments require a very long signal averaging (~ 200 hours are estimated for a bone sample), a synthetically obtained ^{43}Ca-enriched (57.9%) carbonated apatite was used to prepare the sample containing osteocalcin that was used in the 2D MQMAS experiment. The 2D spectrum displays well-resolved spectral lines and clearly shows two high intensity peaks at −0.1 and −6.7 ppm from Ca-I and Ca-II sites in carbonated apatite with a intensity ratio Ca-I:Ca-II=3:4. This observed intensity ratio from the sample containing osteocalcin is similar to that measured from a 5% carbonated apatite powder sample.34 On the other hand, two other relatively lower intensity peaks at 2.4 and 9.5 ppm (see Figure 2b) are also observed from a sample containing osteocalcin; these additional peaks are not present in a 2D spectrum of 5% carbonated apatite powder sample containing no osteocalcin.35 Therefore, the observation of these additional peaks is most likely due to the binding of the bone protein osteocalcin to both calcium sites. The observed significant change in the chemical shift values (−0.1 and −6.7 without and 2.4 and 9.5 ppm with osteocalcin samples)

and the large quadrupole coupling constant (see Table 1) most likely due to the coordination of negatively charged side chains of aspartic acid and carboxylated glutamic acid residues with calcium in a hydroxyapaptite crystal as shown in a previously reported model from a crystallography study.47 However the detailed information about the binding between osteocalcin and carbonated apatite is still limited by the low resolution of ^{43}Ca spectra.

More solid-state NMR experiments such as ^{43}Ca-^{13}C REDOR (Rotaional-Echo Double-Resonance)48 could be performed to obtain the distance between ^{43}Ca in the bone matrix and ^{13}C atoms in the bone protein osteocalcin; since natural-abundance ^{43}Ca-^{1}H REDOR and ^{43}Ca-^{13}C TRAPDOR (TRAnsfer of Population DOuble Resonance) were recently demonstrated, it is possible to use such MAS experiments to measure interatomic distances from bone to understand the protein-calcium interactions in bone.36 In addition, a combination of experimental and quantum chemical calculation approach to characterize the magnitudes of the principal components of ^{43}Ca chemical shift anisotropy tensor and its orientation with respect to quadrupole coupling tensor from model systems to mimic the interaction of calcium sites with bone proteins would provide insights into the coordination chemistry around the calcium sites in bone.37 It may also be fruitful to apply double quantum MAS experiments to extract structural information on the bound osteocalcin, as demonstrated for statherin proteins bound to hydroxyapatite.49–51 Most of these sophisticated solid-state NMR experiments require bone proteins to be labeled with ^{13}C and ^{15}N isotopes and are beyond the scope of this study.

Conclusions

In this study, we have analyzed the calcium coordination environment of bovine cortical bone and model compounds of for bone mineral, including hydroxyapatite and carbonated apatite using ^{43}Ca 1D MAS and 2D 3QMAS NMR experiments. To the best of our knowledge, this study reports the first natural-abundance ^{43}Ca NMR spectrum of a bovine cortical bone specimen sample and it identifies two different calcium sites with a 4:5 ratio. We found that the quadrupole coupling parameters measured from the ^{43}Ca spectrum of the cortical bone sample is significantly larger than that of hydroxyapatite and carbonated apatite due to the presence of additional ions in the cortical bone. We have also demonstrated the use of 2D 3QMAS experiment to probe the interaction of osteocalcin binding with carbonated apatite. Protein-bound and free calcium sites in the sample significantly differ in the observed ^{43}Ca NMR chemical shifts from 2D 3QMAS experiments. We believe that the findings reported in this study will be useful in probing structural changes in the calcium environment accompanying bone mineralization as well as the bone formation processes. This successful demonstration of ^{43}Ca NMR experiments on osteocalcin samples could also enable an investigation of the interaction of non-collagenous bone proteins with bone minerals and organic matrix. We hope that our study would encourage the use of more other cutting-edge solid-state NMR MAS techniques to investigate the high-resolution structure of bone minerals, the interaction between proteins and bone minerals, and the chemical changes in bone. Natural-abundance ^{43}Ca solid-state NMR in general and its applications to structural studies of bone in particular will significantly benefit from the use of highest possible magnetic field NMR spectrometers52, low temperature experiments53, and other successful solid-state NMR techniques.54

Supplementary Material

Refer to Web version on PubMed Central for supplementary material.

Acknowledgments

This research was supported by funds from NIH (S10 RR023597 to A.R., GM084018 to A.R. and AR052010 to M.D.M.,), CRIF-NSF (to the Chemistry Department), DoD/US Army (DAMD17-03-1-0556 to D.H.K), and NIH training grant (R90-DK071506 to N.S). The authors thank Dr. Jeffrey Brender and Dr. Ronald Soong for critical reading of this manuscript.

References

1. Boskey AL. Clin Orthop Relat Res. 1992; 281:244–274. [PubMed: 1323440]
2. Kaplan, FS.; Hayes, WC.; Keaveny, TM.; Boskey, A.; Einhorn, TA.; Iannotti, JP. Formation and Function of Bone. In: Simon, SR., editor. Orthopedic Basic Science. American Academy of Orthopedic Surgeons; Rosemont, Illinois: 1994. p. 127-184.
3. Cho G, Wu Y, Ackerman JL. Science. 2003; 300:1123–1127. [PubMed: 12750514]
4. Wu Y, Ackerman JL, Kim HM, Rey C, Barroug A, Glimcher MJ. J Bone Miner Res. 2002; 17:472–480. [PubMed: 11874238]
5. Zhu P, Xu J, Sahar N, Morris MD, Kohn DH, Ramamoorthy A. J Am Chem Soc. 2009; 131:17064–5. [PubMed: 19894735]
6. Aue WP, Roufosse AH, Glimcher MJ, Griffin RG. Biochemistry. 1984; 23:6110–4. [PubMed: 6525349]
7. Wu Y, Glimcher MJ, Rey C, Ackerman JL. J Mol Biol. 1994; 244:423–35. [PubMed: 7990131]
8. Schick F. Prog Nucl Magn Reson Spectrosc. 1996; 29:169–227.
9. Wilson EE, Awonusi A, Morris MD, Kohn DH, Tecklenburg MMJ, Beck LW. Biophys J. 2006; 90:3722–3731. [PubMed: 16500963]
10. Kolodziejski W. Topics in Current Chemistry. 2004; 246:235–270.
11. Yesinowski JP, Eckert H. J Am Chem Soc. 1987; 109:6274–6282.
12. Santos RA, Wind RA, Bronnimann CE. J Magn Reson. 1994; B105:183–187.
13. Duer MJ, Friscic T, Murray RC, Reid DG, Wise ER. Biophys J. 2009; 96:3372–3378. [PubMed: 19383480]
14. Wise ER, Maltsev S, Davies ME, Duer MJ, Jaeger C, Loveridge N, Murray RC, Reid DG. Chem Mater. 2007; 19:5055–5057.
15. Beshah K, Rey C, Glimcher MJ, Schimizu M, Griffin RG. J Solid State Chem. 1990; 84:71–81.
16. Huster D, Schiller J, Arnold K. Magn Reson Med. 2002; 48:624–632. [PubMed: 12353279]
17. Tseng YH, Mou CY, Chan CC. J Am Chem Soc. 2006; 128:6909–6918. [PubMed: 16719471]
18. Wu Y, Ackerman JL, Kim HM, Rey C, Barroug A, Glimcher MJ. J Bone Miner Res. 2002; 17:472–480. [PubMed: 11874238]
19. Mukherjee S, Song Y, Oldfield E. J Am Chem Soc. 2008; 130:1264–1273. [PubMed: 18173269]
20. Mukherjee S, Huang C, Guerra F, Wang K, Oldfield E. J Am Chem Soc. 2008; 130:1264–1273. [PubMed: 18173269]
21. Kaflak-Hachulska A, Samoson A, Kolodziejski W. Calcif Tissue Int. 2003; 73:476–486. [PubMed: 12958695]
22. Nancollas GH, Tang R, Phipps RJ, Henneman Z, Gulde S, Wu W, Mangood A, Russell RG, Ebetino FH. Bone. 2006; 38:617. [PubMed: 16046206]
23. Urry DW, Trapane TL, Venkatachalam CM. Calcif Tissue Int. 1982; 34:S41–S46.15. [PubMed: 6816453]
24. Vogel HJ, Andersson T, Braunlin WH, Drakenberg T, Forsen S. Biochem Biophys Res Commun. 1984; 122:1350–1356. [PubMed: 6477566]
25. Drakenberg T, Andersson T, Forsn S, Wieloch T. Biochemistry. 1984; 23:2387–2392. [PubMed: 6477872]
26. Braunlin WH, Vogel HJ, Drakenberg T, Bennick A. Biochemistry. 1986; 25:584–589. [PubMed: 3955015]
27. Drakenberg T, Johansson C, Forsen S. Methods Mol Biol. 1997; 60:299. [PubMed: 9276252]

28. Aramini JM, Drakenberg T, Hiraoki T, Ke Y, Nitta K, Vogel HJ. Biochemistry. 1992; 31:6761–6768. [PubMed: 1637811]
29. Drakenberg T. Methods Mol Biol. 2002; 173:217–230. [PubMed: 11859764]
30. Aramini JM, Vogel HJ. Biochem Cell Biol. 1998; 76:210. [PubMed: 9923690]
31. Forsen S, Johansson C, Linse S. Methods Enzymol. 1993; 227:107. [PubMed: 8255223]
32. Shimoda K, Tobu Y, Shimoikeda Y, Nemoto T, Saito K. J Magn Reson. 2007; 186:156–159. [PubMed: 17306578]
33. Wong A, Howes AP, Dupree R, Smith ME. Chem Phys Lett. 2006; 427:201–205.
34. Laurencin D, Wong A, Dupree R, Smith ME. Magn Reson Chem. 2008; 46:347. [PubMed: 18306258]
35. Laurencin D, Wong A, Hanna JV, Dupree R, Smith ME. J Am Chem Soc. 2008; 130:2412. [PubMed: 18237175]
36. Laurencin D, Gervais C, Wong A, Coelho C, Mauri F, Massiot D, Smith ME, Bonhomme C. J Am Chem Soc. 2009; 131:13430. [PubMed: 19715269]
37. Bryce DL, Bultz EB, Aebi D. J Am Chem Soc. 2008; 130:9282. [PubMed: 18576634]
38. Lin ZJ, Smith ME, Sowrey FE, Newport RJ. Phys Rev B. 2004; 69:224107–224113.
39. Carden A, Rajachar RM, Morris MD, Kohn DH. Calcif Tissue Int. 2003; 72:166–175. [PubMed: 12469250]
40. Penel G, Leroy G, Rey C, Bres E. Calcif Tissue Int. 1998; 63:475–481. [PubMed: 9817941]
41. Awonusi A, Morris MD, Tecklenburg MMJ. Calcif Tissue Int. 2007; 81:46–52. [PubMed: 17551767]
42. Morris, MD.; Schulmerich, MV.; Dooley, KA.; Esmonde-White, KA. Infrared and Raman Spectroscopic Imaging. Salzer, R.; Siesler, HW., editors. Wiley-VCH, GmbH & Co, KGaA; Weimheim: 2009. p. 149-172.
43. Termine JD, Eanes ED, Greenfield DJ, Nylen MU, Harper RA. Calcif Tissue Res. 1973; 12:73–82. [PubMed: 4701457]
44. Featherstone JDB, Pearson S, LeGeros RZ. Caries Res. 1984; 18:63–66. [PubMed: 6580956]
45. Kemp TF, Smith ME. Solid State Nucl Magn Reson. 2009; 35:243. [PubMed: 19186033]
46. Frydman L, Harwood JS. J Am Chem Soc. 1995; 117:5367.
47. Hoang QQ, Sicheri F, Howard AJ, Yang DSC. Nature. 2003; 425:977–980. [PubMed: 14586470]
48. Gullion T, Schaefer J. J Magn Reson. 1989; 81:196–200.
49. Gibson JM, Raghunathan V, Popham JM, Stayton PS, Drobny GP. J Am Chem Soc. 2005; 127:9350. [PubMed: 15984845]
50. Drobny GP, Long JR, Karlsson T, Shaw W, Popham J, Oyler N, Bower P, Stringer J, Gregory D, Mehta M, Stayton PS. Annu Rev Phys Chem. 2003; 54:531–71. [PubMed: 12709513]
51. Goobes G, Goobes R, Schueler-Furman O, Baker D, Stayton PS, Drobny GP. Proc Natl Acad Sci U S A. 2006; 103:16083–16088. [PubMed: 17060618]
52. Hung I, Shetty K, Ellis PD, Brey WW, Gan ZH. Solid State Nucl Magn Reson. 2009; 36:159–163. [PubMed: 19913391]
53. Lipton AS, Heck RW, de Jong WA, Gao AR, Wu XJ, Roehrich A, Harbison GS, Ellis PD. J Am Chem Soc. 2009; 131:13992–13999. [PubMed: 19746904]
54. Fujiwara T, Ramamoorthy A. Ann Rep NMR Spectrosc. 2006; 58:155–175.

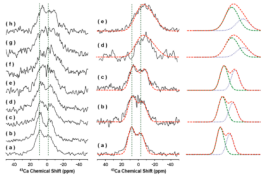

Figure 1. Natural-abundance ^{43}Ca NMR spectra of powder samples of bone and model compounds

First column: Natural-abundance ^{43}Ca NMR spectra of (a) 0%, (b) 0.3%, (c) 2.3%, (d) 3.5%, (e) 5.0%, (f) 6.9%, (g) 8.8%, and (h) 10% carbonated apatite samples. Second column: Natural-abundance ^{43}Ca NMR spectra of (a) hydroxyapatite, (b) 5% carbonated apatite, (c) 10% carbonated apatite, (d) deproteined cortical bone, and (e) cortical bone samples. Spectra were obtained on a 833 MHz solid-state NMR spectrometer using a single-resonance 4 mm MAS probe with a spinning frequency of 10 kHz at room temperature. All spectra were recorded using a spin-echo, 90°-τ-180°-τ-acquire, sequence with a 2 μs 90° pulse width, τ of 40 μs, and a 0.5 s recycle delay. 131,072 scans were used for figures a–d, while 480,000 and 262,144 scans were used for the deproteined bone (d) and cortical bone (e) spectra, respectively. A saturated solution of $CaCl_2$ (at 0 ppm) was used as a standard to reference ^{43}Ca chemical shift. The simulated spectra are displayed in red dashed lines (second and third columns). The simulated Ca-II (green) and Ca-I (blue) are also plotted for a comparison (in the third column).

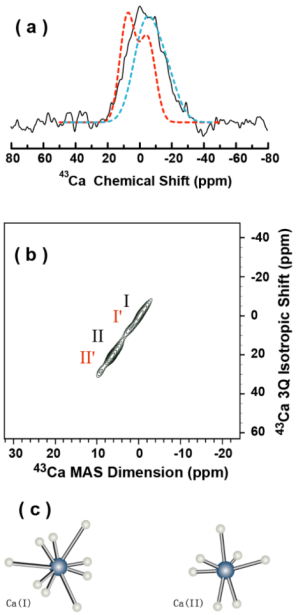

Figure 2. Calcium-43 MAS experiments probing the interaction of osteocalcin bone protein with calcium sites in 5 % carbonated apatite

(a) One-dimensional ^{43}Ca MAS spectrum of ^{43}Ca-enriched carbonated apatite containing osteocalcin protein at room temperature (solid line in black), simulated spectrum of 5% carbonated apatite (dashed lines in red color; same as in Figure 1b of the second column), and simulated spectrum of cortical bone (dashed lines in blue color; same as in Figure 1e of the second column). (b) Two-dimensional MQMAS spectrum that correlates the ^{43}Ca chemical shift and a triple-quantum frequency of ^{43}Ca-enriched carbonated apatite powder sample containing osteocalcin protein at room temperature. 5 and 10 μs were the length of the excitation and the conversion radio frequency pulses, respectively. The 2D spectrum is the resultant of 16 t1 experiments, 61440 scans, a 0.5 s recycle delay, and a 10 kHz sample spinning speed. The 1D spectrum was obtained using a single pulse sequence with a 90° pulse length of 2 μs, 512000 scans, a recycle delay of 250 ms, and a 10 kHz sample spinning speed. (c) The two calcium coordination environments in carbonated apatite.

Table 1

NMR parameters (isotropic chemical shift, δ_{iso}, quadrupole coupling constant, C_Q, and asymmetry parameter, η_Q) obtained from a comparison of experimental and simulated ^{43}Ca MAS spectra of hydroxyapatite, carbonated apatite and bovine cortical bone samples.

	δ_{iso}(ppm)	C_Q(MHz)	η_Q
Hydroxyapatite:			
Ca II	14	2.6	0.6
Ca I	2	2.6	0.4
Carbonated apatite (5%):			
Ca II	13	2.6	0.6
Ca I	0	2.6	0.4
Carbonated apatite (10%):			
Ca II	11.5	2.6	0.6
Ca I	−2	2.6	0.4
Bovine cortical bone:			
Ca II	10	4	0.6
Ca I	−2	4	0.4